

## Single-step chemical synthesis of ferrite hollow nanospheres

This article has been downloaded from IOPscience. Please scroll down to see the full text article.

2009 Nanotechnology 20 045606

(<http://iopscience.iop.org/0957-4484/20/4/045606>)

The Table of Contents and more related content is available

Download details:

IP Address: 155.210.234.214

The article was downloaded on 20/12/2008 at 17:51

Please note that terms and conditions apply.

# Single-step chemical synthesis of ferrite hollow nanospheres

Enio Lima Jr<sup>1</sup>, José M Vargas<sup>1,6</sup>, Roberto D Zysler<sup>1,7</sup>,  
Hercilio R Rechenberg<sup>2</sup>, Renato Cohen<sup>2</sup>, Jordi Arbiol<sup>3</sup>,  
Gerardo F Goya<sup>4</sup>, Alfonso Ibarra<sup>4</sup> and M Ricardo Ibarra<sup>4,5</sup>

<sup>1</sup> Centro Atómico Bariloche and Instituto Balseiro, 8400 SC de Bariloche, RN, Argentina

<sup>2</sup> Instituto de Física, Universidade de São Paulo, 05315-970 São Paulo, SP, Brazil

<sup>3</sup> GAEN-CeMARC, Group of Advanced Electron Nanoscopy—Centre de Microscopia d'Alta Resolució de Catalunya, Universitat de Barcelona, E-08028 Barcelona, CAT, Spain

<sup>4</sup> Instituto de Nanociencia de Aragón, Universidad de Zaragoza, E-50009 Zaragoza, Spain

<sup>5</sup> Instituto de Ciencia de Materiales de Aragón, Universidad de Zaragoza-CSIC, E-50009 Zaragoza, Spain

E-mail: [zysler@cab.cnea.gov.ar](mailto:zysler@cab.cnea.gov.ar)

Received 10 October 2008, in final form 14 November 2008

Published 19 December 2008

Online at [stacks.iop.org/Nano/20/045606](http://stacks.iop.org/Nano/20/045606)

## Abstract

We report a single-step chemical synthesis of iron oxide hollow nanospheres with 9.3 nm in diameter. The sample presents a narrow particle diameter distribution and chemical homogeneity. The hollow nature of the particles is confirmed by HRTEM and HAADF STEM analysis. Electron and x-ray diffraction show that the outer material component is constituted by 2 nm ferrite crystals. Mössbauer data provide further evidence for the formation of iron oxide with high structural disorder, magnetically ordered at 4.2 K and superparamagnetism at room temperature. An unusual magnetic behavior under an applied field is reported, which can be explained by the large fraction of atoms existing at both inner and outer surfaces.

 Supplementary data are available from [stacks.iop.org/Nano/20/045606](http://stacks.iop.org/Nano/20/045606)

(Some figures in this article are in colour only in the electronic version)

## 1. Introduction

Finite-size effects occur in nanostructured materials as thin films, nanoparticles (NP) and nanowires. The control of their morphology and functionalities on the nanoscale is a prerequisite for some applications. magnetic nanoparticles as nanovectors for drug delivery [1, 2]. Spherical empty nanocapsules are appealing for such applications since they could store larger amounts of drug than solid NPs of the same size. On the basis of their enhanced surface/bulk atomic ratio, magnetic hollow nanospheres (HNS) provide an excellent system to study the competition between surface and bulk magnetism at the nanoscale level and open up new perspectives for experimental and theoretical developments. The magnetic behavior of the surface atoms is characterized by the lack of

symmetry and broken chemical and exchange bonds which introduce structural and magnetic disorder and originate an enhancement of the site-by-site magnetic anisotropy [3–5].

Semiconductor and magnetic micro-, submicro- and nanospheres have already been reported in the literature, being produced by different techniques with distinct morphological characteristics, as mentioned in the review of Gubin *et al* [6]. Regarding the iron oxides, HNS with narrow diameter dispersion were produced by a controlled post-synthesis oxidization of Fe or Fe<sub>3</sub>O<sub>4</sub> nanoparticles [7]. In a similar way, Yin *et al* have produced CoO, CoSe and CoS nanoparticles with diameters of 20 nm and a 4–5 nm thick shell [8]. In this kind of procedure, the hollow spheres are formed by Fe and Co diffusion to the outer part of the particle during the oxidization. Cabot *et al* showed that hollow iron oxide nanoparticles are formed by this mechanism within a large intermediate temperature range ( $T < 523$  K) [9]. The magnetic properties of these systems have so far only been partially explored. It is known that the post-synthesis oxidization process influences

<sup>6</sup> Present address: Instituto de Física Gleb Wataghin, Universidade de Campinas, Brazil.

<sup>7</sup> Author to whom any correspondence should be addressed.

the magnetic behavior related to the core/surface structure by increasing the crystalline order of the system. In this way, a single-step and controlled procedure to synthesized magnetic HNS has the potential to produce systems with particular magnetic properties. Here, we report a single-step method for obtaining monodisperse ferrite HNS, with no subsequent oxidization process. As a consequence of the single-step synthesis, our samples have high crystalline disorder degree and consequently present unusual magnetic behavior related to the large surface/bulk atomic ratio due to both inner and outer surfaces of a hollow sphere.

## 2. Sample preparation

Ferrite HNS were prepared by the high temperature (543 K) decomposition of  $\text{Fe}(\text{acac})_3$  in the presence of 1,2-hexadecanediol (a long-chain alcohol), and the surfactants oleic acid and oleylamine as described by Sun *et al* [10] and Vargas *et al* [11]. The precursor:alcohol:surfactant molar ratio was 1:1:9. The solvent was phenyl ether with boiling point at 543 K. Our synthesis procedure started at the reflux condition (543 K) in argon flux ( $\sim 500 \text{ cm}^3 \text{ min}^{-1}$ ), and after  $\sim 5$  min the temperature was slowly cooled down to 473 K over 30 min. This temperature is below the higher limit of the temperature regime where the iron oxide HNS are spontaneously produced according to Cabot *et al* [9]. The synthesized HNS were precipitated by adding ethanol (250 ml) to the bath followed by 20 min centrifugation at 7000 rpm. The HNS are coated by the surfactant molecules, preventing agglomeration and increasing the chemical stability of the surface.

## 3. Results and discussion

The morphology and structure of the particles are studied by using high-resolution TEM (HRTEM) combined with STEM in high angular annular dark-field (HAADF) and bright-field (BFSTEM) modes. Particle composition was carried out by means of electron energy-loss spectroscopy (EELS) as well as energy-filtered TEM (EFTEM). The samples were prepared by dropping a colloidal suspension of HNS onto a carbon-coated copper grid. Low-resolution images of the sample (figure 1(a)) show a highly homogeneous lognormal distribution of particles of mean diameter  $\langle d \rangle = 9.3 \text{ nm}$ , with standard deviation  $\sigma = 0.27$  (see the histogram in the inset of figure 1(a)). HAADF images clearly show (figure 1(b)) that the inner region of the spheres has a lower density than the outer one; however, the intensity in the inner part is higher than in the area between particles, reflecting the hollow nature of the particles. The profile analysis (figure 1(c)), made over the bar of figure 1(b)) confirms a decrease of the material density at the inner part of the particle projection. The HAADF profile of a particle with homogeneous density is proportional to  $Z^2$  and the thickness at every projected point. The experimental HAADF profile exhibited in figure 1(c) (squares) is well fitted by a calculated profile (solid line) taking into account the spherical geometry and the homogeneous density of the system and considering a particle diameter of 9.3 nm and an inner diameter of 2.8 nm, i.e. we have calculated the expected profile of a sphere with a

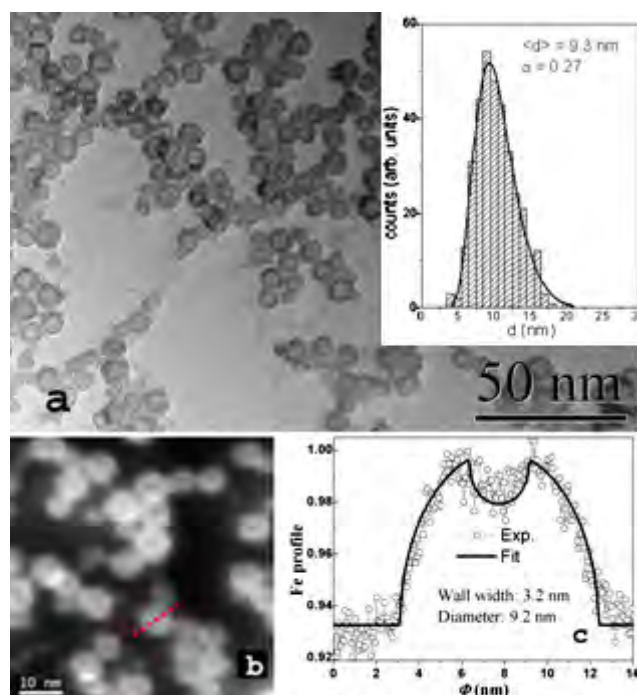


**Figure 1.** (a) TEM image of synthesized HNS with  $\langle d \rangle = 9.3 \text{ nm}$  and low dispersion  $\sigma = 0.27$  (inset: histogram of particle diameters of several TEM images). (b) HAADF STEM image of our nanoparticles and (c) HAADF profile through one nanoparticle (open circles) fitted with a model of a hollow particle (solid line).

diameter of 9.3 nm and subtracted the profile of a sphere with a diameter of 2.8 nm. We have performed similar HAADF analysis for other regions of our samples, observing always hollow nanoparticles with similar profiles with inner diameters varying from 2.5 to 3.2 nm. The small discrepancy between calculated and experimental HAADF profiles are related to the shell (outer region) of the spheres being constituted by crystals with distinct sizes, as discussed in the HRTEM analysis. This being the simplest model, a more complete calculation would include both inhomogeneity effects and/or the presence of roughness/grain boundaries.

HRTEM micrographs (figure 2(a)) reveal the polycrystalline nature of the shell region with no preferential orientation, which is more evident in the magnified particle in figure 2(d). It is important to point out that, depending on the defocus, crystal planes were observed either on the external part or on the top of the inner part. This fact discards the existence of toroidal-like structures. Fast Fourier transformation (FFT) or power spectra of the HRTEM image of a single HNS (figure 2(b)) is hard to index as a consequence of its polycrystalline nature, but the majority of the spots are related to the spinel structure of magnetite/maghemite ( $\text{Fe}_3\text{O}_4/\gamma\text{-Fe}_2\text{O}_3$ ), although some spots observed are closer to the  $d$  spacing of the hematite ( $\alpha\text{-Fe}_2\text{O}_3$ ). The x-ray diffraction peak (figure 2(c)) corresponds to the (311) plane of magnetite or maghemite. It is consistent with the iron oxide spinel structure obtained from the power spectra of the magnified HRTEM image of a single crystal (figure 2(d)), indicating in both cases a spinel structure with  $d$  spacing close to that of

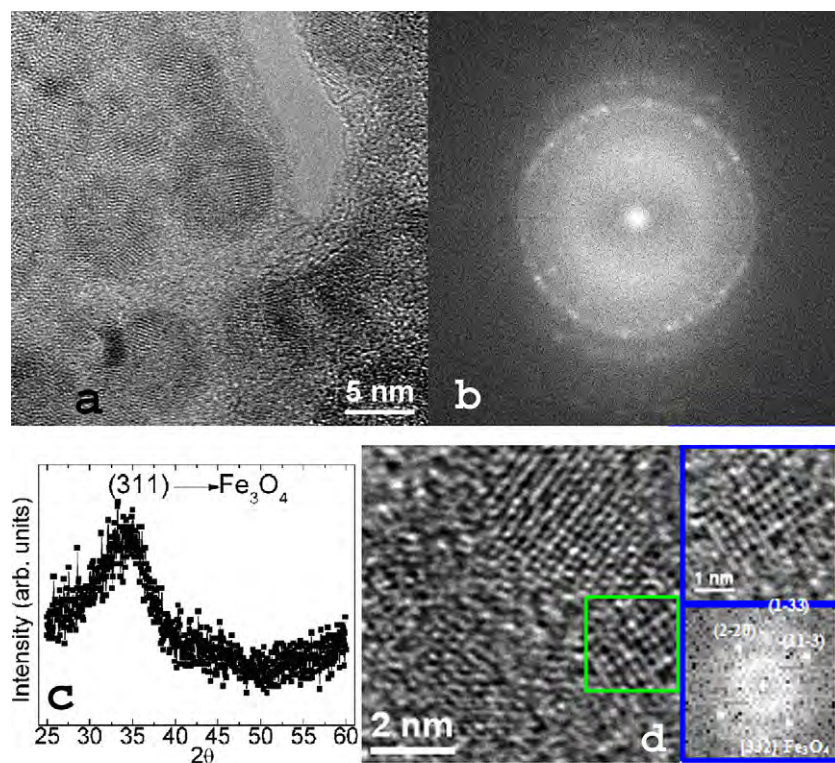


**Figure 2.** (a) HRTEM micrograph and (b) corresponding powder spectrum (FFT) of HNS. (c) X-ray profile of our HNS with a broad diffraction peak at the position expected for the (311) plane of ferrite structure. (d) HRTEM micrograph of a single HNS. At the top right corner we show a magnified HRTEM image of one single crystal in the shell of HNS and the respective power spectrum indexed with the spinel structure.

bulk ferrite ( $d = 0.2532$  nm) [12]. Furthermore, the x-ray line broadening reflects crystallite sizes of 2 nm, in agreement with the diameter of the grains in the HNS observed by HRTEM.

All these results are in agreement with the hollow nature of the particles observed. Moreover, BFTEM micrographs at high tilt angle ( $35^\circ$ ) do not show changes in the observed projection denoting an invariable morphology under particle rotation, supporting the hypothesis that our nanostructures are HNS with a polycrystalline shell constituted by ferrite nanocrystals with 2–3 nm. EELS and EFTEM analysis (not shown) revealed that the elements composing the nanospheres were only Fe and O.

Considering the polycrystalline nature of the nanoparticles and the single-step synthesis method of our HNS, it is expected that the growth mechanism should be distinct from that of the post-synthesis oxidizing method [7–9]. However, we do not fully understand the growth mechanism of these HNS going on during our synthesis, having only indications about it. The polycrystalline nature of our HNS, constituted by 2–3 nm crystallites, may suggest that they are formed by the assembly of small particles (2–3 nm) seeded in the first step of the synthesis (5 min at reflux condition), and the HNS forms in the subsequent step when the temperature is slowly reduced to 473 K. Those seeds (i.e. small nanoparticles of 2–3 nm) which are not incorporated into the HNS structure are removed during subsequent centrifugation and washing procedures, so they are no longer present in TEM or HRTEM images. We have also performed two synthesis tests to explore some ideas about the growth mechanism of our HNS. First, a new synthesis

was carried out using the same amount of reagents, but keeping the system in reflux condition for 2 h, resulting in filled  $\text{Fe}_3\text{O}_4$  nanoparticles of  $\sim 7$  nm diameter and high crystallinity. In this way, we can infer that the prolonged time at high temperature induces an increase in the size of the seed or the coalescence of the formed hollow particles. In the second test the phenyl ether was replaced by trioctylamine (boiling point 638 K). For a sample prepared in 20 min, we observe highly crystalline particles with  $\sim 20$  nm or  $\sim 10$  nm diameters. We also observe some  $\sim 20$  nm HNS (5 nm shell width) together with structures formed by the fusion or percolation of two crystallites. A 30 min synthesis leads only to cubic crystalline nanoparticles of spinel structure with  $\langle d \rangle = 20$ –24 nm. This second test also suggests that long times and large temperatures lead to the formation of filled and larger particles by the fusion of smaller ones. The whole picture suggests that our HNS may be formed by the percolation of small seeds with  $\sim 2$ –3 nm. This hypothesis about the growth mechanism of our HNS needs to be confirmed by a comprehensive study concerning all synthesis conditions and parameters, but this task is beyond the scope of the present work.

Mössbauer spectra (MS) of our sample were collected at 4.2–300 K in a liquid He flow cryostat with a conventional constant-acceleration spectrometer in transmission geometry using a  $^{57}\text{Co}/\text{Rh}$  source. The room-temperature MS spectrum (supplementary material available at [stacks.iop.org/Nano/20/045606](http://stacks.iop.org/Nano/20/045606)) is a doublet associated with the SPM state of the system with narrow lines (linewidth

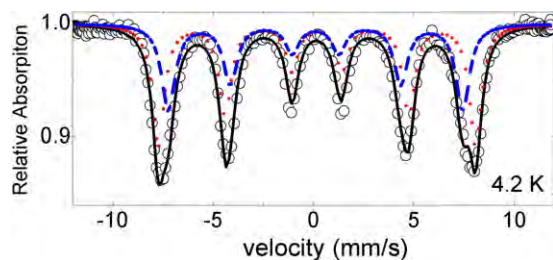


**Figure 3.** Mössbauer spectrum of HNS collected at 4.2 K. Solid line is the fitted spectrum and dashed red and dotted blue lines are the subspectra referring to sites A and B, respectively.

$w = 0.65 \text{ mm s}^{-1}$ ), isomer shift  $IS = 0.36 \text{ mm s}^{-1}$  and quadrupolar splitting  $QS = 0.98 \text{ mm s}^{-1}$ . The IS value is similar to the one commonly observed in  $\text{Fe}^{3+}$  ferrites in the SPM regime [13]. However, the QS value is much larger than expected for these materials [14–16], reflecting a local symmetry lower than cubic, implying broken Fe–Fe superexchange paths and/or oxygen vacancies located at both inner and outer surfaces. This is in agreement with previous results on highly disordered ferrites obtained from ball-milling, which show QS values similar to the present ones [17, 18]. At 4.2 K (figure 3) the relaxation time is slow enough to ensure a static hyperfine splitting, and the spectrum was fitted with two sextets. The obtained mean hyperfine field values ( $B_{\text{hf}} = 49.1$  and  $45.5 \text{ T}$ ) are smaller than those observed for A and B sites in ferrite nanoparticles [19]. To ensure that these parameters could be associated with the iron oxide phase, a thermal treatment of the HNS was performed at 573 K for 30 min in pure argon flow. This annealing temperature is below the decomposition temperature of oleic acid; thus, HNS agglomeration was still prevented during the thermal treatment. Moreover, the low annealing temperature and inert atmosphere ruled out the possibility of Fe reduction or oxidation, so only structural changes were expected to be induced by the treatment. HRTEM analysis confirms the absence of the inner cavity in the annealed sample, as shown in the supplementary material (available at [stacks.iop.org/Nano/20/045606](http://stacks.iop.org/Nano/20/045606)). The filled nanoparticles of the annealed sample have smaller sizes and a narrower size distribution ( $\langle d \rangle = 6.3 \text{ nm}$ ,  $\sigma = 0.22$ ). MS spectroscopy performed at 4.2 K (supplementary material available at [stacks.iop.org/Nano/20/045606](http://stacks.iop.org/Nano/20/045606)) on the annealed sample indicated that ferrite is the only iron-containing phase in the annealed system. The two sextets associated with the magnetic sublattices A and B with  $B_{\text{hf}} = 53.3$  and  $50.5 \text{ T}$  are characteristic of the magnetite. Thus, on the assumption that no chemical changes were induced by the thermal treatment, we conclude that our HNS are composed of an iron oxide phase containing  $\text{Fe}^{2+}$  and  $\text{Fe}^{3+}$  ions, probably a non-stoichiometric magnetite. The smaller hyperfine field values found in the as-made HNS Mössbauer spectrum could be attributed to the collective thermal relaxation of the moments in association with the reduction of the magnetic anisotropy energy barrier  $E_a$  [20]. This anomalous small  $E_a$  value, in comparison to that expected for 9.3 nm ferrite nanoparticles, could be explained on the basis of the structural disorder of the inner and outer surfaces of the HNS. The large linewidth values of

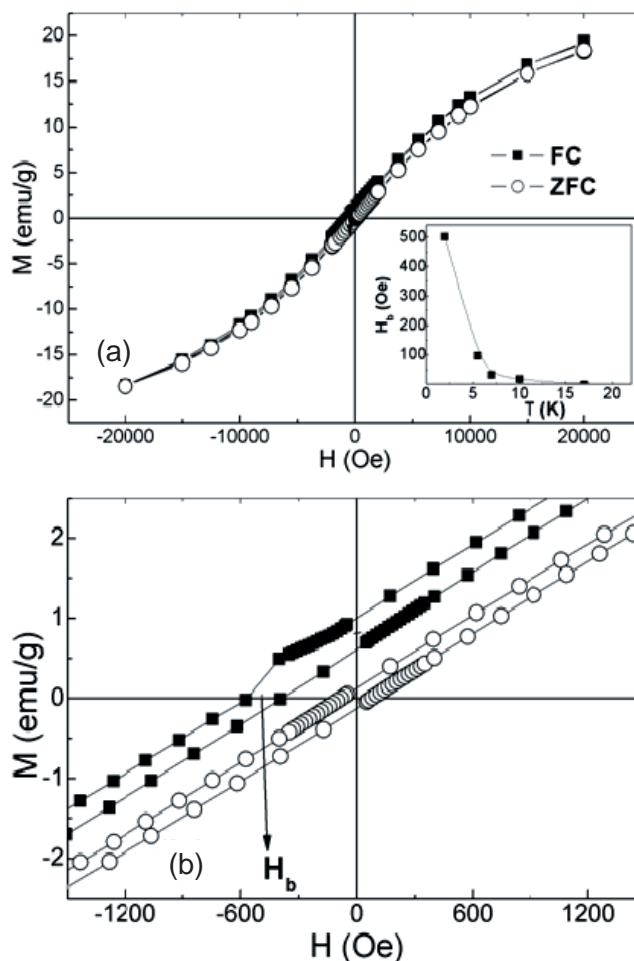


**Figure 4.** (a) Magnetization isotherms (in ZFC and FC modes) measured at  $T = 2 \text{ K}$  and up to 20 kOe. Top inset: thermal dependence of the bias field  $H_b(T)$  obtained from the FC  $M(H)$  results. (b) Low-field region of  $M(H)$  curves showing in detail the FC loop shift.

the magnetic sextets in the 4.2 K MS spectrum of HNS also indicate a locally distorted environment of the Fe ions.

The structural disorder present in our HNS associated with inner and outer surfaces, together with the high surface/volume ratio, gives rise to unusual magnetic properties. Figure 4(a) shows the magnetization loops measured in the ZFC and FC conditions at 2 K (cooling field 10 kOe). ZFC loops show a very low coercive field  $H_C$  (see in detail the low-field region in figure 4(b)) compared to what is usually observed in ferrite nanoparticles [21], and no magnetic saturation occurs up to 20 kOe ( $\sim 19 \text{ emu g}^{-1}$ ). We also have observed a significant loop shift in the FC cycle at temperatures below 20 K (see a magnification of the low-field part of the hysteresis loop in figure 4(b)). The bias field,  $H_b$ , is defined as the center field of the shifted magnetic loop and it exhibits a clear thermal dependence (see the inset of figure 4(a)), being about 500 Oe at 2 K. Actually, the FC loop is shifted upwards with respect to the ZFC loop, as a remanent moment is acting to increase the FC magnetization in the whole field range. A possibility for this unusual magnetic behavior would be the formation of an antiferromagnetic iron

oxide phase on inner and outer surfaces [22]. However, the hysteresis loop of the annealed sample recovers the characteristics expected for magnetite nanoparticles: low irreversibility field, linear dependence of the coercive field with  $T^{1/2}$  (as expected for the Stoner–Wohlfarth model),  $H_C \sim 850$  Oe and  $M_S \sim 56$  emu g<sup>-1</sup> at 4.2 K. Moreover, no shift was observed in the FC loop (supplementary material available at [stacks.iop.org/Nano/20/045606](http://stacks.iop.org/Nano/20/045606)). Therefore, the unusual magnetic properties observed for our HNS are related to the morphology and crystalline structure of the system. The existence of the inner and outer surfaces magnetically disordered in the HNS are responsible for the strong irreversibility observed in the ZFC and FC processes.

Although the magnetic behavior of our HNS at low temperature is clearly unusual, more analysis involving magnetization measurements and in-field Mössbauer spectroscopy, as well as Monte Carlo simulations, are necessary to elucidate its origin. This extension of the present work is under way.

#### 4. Conclusions

In summary, we propose a new synthesis method to obtain ferrite hollow nanospheres with less than 10 nm mean diameter and a thickness of  $\sim 3$  nm by means of a single-step chemical method with no post-synthesis oxidizing process. As a consequence, the system exhibits a large amount of structural disorder manifested by the electron microscopy techniques. The magnetic characterization of these nanostructures brings about relevant phenomena associated with their particular morphology.

#### Acknowledgments

We are grateful to Professors J Nogués and P A Algarabel for critical reading and discussion of this manuscript. We also acknowledge Professor L M Rossi for the TEM image in the supplementary material (available at [stacks.iop.org/Nano/20/045606](http://stacks.iop.org/Nano/20/045606)). This work received financial support from the Argentinian agencies ANPCyT, CONICET

and UNCuyo, the Spanish MEC under grants NAN2006-26646-E and Consolider CSD2006-12, and the Brazilian agencies FAPESP and CNPq. GFG acknowledges support from the Spanish MEC through the Ramon y Cajal program. EL Jr and JMV acknowledge fellowships from FAPESP.

#### References

- [1] Arruebo M, Fernandez-Pacheco R, Ibarra M R and Santamaría J 2007 *Nano Today* **2** 23
- [2] Goya G F, Grazú V and Ibarra M R 2008 *Curr. Nanosci.* **4** 1
- [3] Martinez B, Obradors X, Balcells L I, Rouanet A and Monty C 1998 *Phys. Rev. Lett.* **80** 181
- [4] Battle X and Labarta A 2002 *J. Phys. D: Appl. Phys.* **35** R15
- [5] Kodama R H and Berkowitz A E 1999 *Phys. Rev. B* **59** 6321
- [6] Gubin S P, Yurkov G Yu and Kataeva N A 2005 *Inorg. Mater.* **41** 1017
- [7] Peng S and Sun S 2007 *Angew. Chem. Int. Edn* **46** 4155
- [8] Yin Y, Rioux R M, Erdonmez C K, Hughes S, Somorjai G A and Alivisatos A P 2004 *Science* **304** 711
- [9] Cabot A, Puentes V F, Shevchenko E, Yin Y, Balcells L, Marcus M A, Hughes S M and Alivisatos A P 2007 *J. Am. Chem. Soc.* **129** 10358
- [10] Sun S, Zeng H, Robinson D B, Raoux S, Rice P M, Wang S X and Li G 2004 *J. Am. Chem. Soc.* **126** 273
- [11] Vargas J M and Zysler R D 2005 *Nanotechnology* **16** 1474
- [12] Cornell R M and Schwetmann U 1996 *The Iron Oxides: Structure, Properties, Reactions, Occurrence and Use* (Weinheim: VCH) chapter 7, pp 166–7
- [13] Goya G F, Berquó T S, Fonseca F C and Morales M P 2003 *J. Appl. Phys.* **94** 9520
- [14] Voigt F C, Palstra T T M, Niesen L, Rogojuanu O C, James M A and Hibma T 1998 *Phys. Rev. B* **57** R8107
- [15] Goya G F 2002 *IEEE Trans. Magn.* **38** 127
- [16] Culita D C, Marinescu G, Patron L, Carpa O, Cizmas C B and Diamandescu L 2008 *Mater. Chem. Phys.* **111** 381
- [17] Bao L and Jiang J S 2005 *Physica B* **367** 182
- [18] Goya G F and Rechenberg H R 2002 *Mater. Sci. Forum* **403** 127
- [19] Arelaro A D, Lima E Jr, Rossi L M, Kyohara P K and Rechenberg H R 2008 *J. Magn. Magn. Mater.* **320** e335
- [20] Mórup S 1983 *J. Magn. Magn. Mater.* **37** 39
- [21] Lima E Jr, Brandl A L, Arelaro A D and Goya G F 2006 *J. Appl. Phys.* **99** 083908
- [22] Nogués J, Sort J, Langlais V, Skumryev V, Suriñach S, Muñoz J S and Baró M D 2005 *Phys. Rep.* **422** 65